

# The Effect of Enzymatic Reaction on Dissolution Rate: Theoretical Analysis and Experimental Test

DONALD A. JOHNSON AND GORDON L. AMIDON\*

Received June 21, 1985, from the College of Pharmacy, The University of Michigan, Ann Arbor, MI 48109-1065. Accepted for publication November 13, 1985.

**Abstract** □ The dissolution behavior of *N*-acetylphenylalanine ethyl ester (1) and *N*-benzoyltyrosine ethyl ester (2) from a rotating disk into aqueous solutions containing the enzyme  $\alpha$ -chymotrypsin was investigated. The effect of the bulk enzymatic reaction on the dissolution rates is modeled using the continuity equation where the reaction term is considered a constant throughout the reaction zone. Dimensional analysis on the continuity equation defines the important parameter  $R^* = K_{cat}E_0h^2/(C_sD)$  which is the ratio of the diffusion time to the reaction time. This parameter correctly predicted the fact that the enzymatic reaction had only a slight impact on the dissolution of the highly soluble 1 while the effect on the less soluble 2 was large. Also predicted by  $R^*$  is the dissolution dependence on the catalytic rate constant. The variation of this rate constant with pH is consistent with the dependence on pH found for the dissolution rate of 2. It is further demonstrated that the decrease in dissolution rate with solubility can be significantly reduced when the dissolving compound is an enzyme substrate. For the two compounds used in this study the dissolution rate decreased with the square root of solubility, as predicted by the theoretical analysis in the presence of enzyme. Other experiments included the variation of the enzyme concentration and the rotational speed of the spinning disk. All experiments were designed to show how  $R^*$  could correctly predict the relative importance of the convective, diffusive, and reactive processes.

The effect of a drug chemically reacting subsequent to its dissolution can greatly affect the dissolution rate.<sup>1-12</sup> Studies have included the dissolution and subsequent hydrolysis of the two theophylline prodrugs 7-acetyltheophylline and 7,7'-succinyliditheophylline<sup>3,7</sup> as well as the dissolution and enzymatic hydrolysis of chloramphenicol palmitate.<sup>4</sup> Other studies were concerned with the effect of complexation with caffeine upon dissolution of benzoic acid<sup>11</sup> and salicylamide.<sup>6</sup> Dissolution rates of cholesterol have also been found to be dependent on the type and amount of bile acid present in the dissolution media.<sup>12</sup>

The effect of reaction on the dissolution rate is of particular significance when the drug is a weak acid or base.<sup>1,2,8-10</sup> This is due to the fact that acid/base reaction kinetics are usually rapid compared with diffusion kinetics.

Aqueous hydrolysis of amides or esters is not normally as fast as acid/base reactions. Therefore, aqueous hydrolysis is not expected to affect the dissolution rates of amides or esters. If, however, the amide or ester is an amino acid derivative which is also an enzyme substrate, aminolysis or esterolysis may affect dissolution rates since enzyme catalytic rate constants can be quite large. It may be possible, therefore, to make an amino acid prodrug suspension which is pharmaceutically stable yet undergoes rapid dissolution and bioconversion by one of the digestive enzymes upon oral administration.<sup>13</sup>

In order to determine how fast an enzymatic reaction must be in order to affect dissolution rates, one can compare the dissolution rate and subsequent diffusion through a film with the rate of mass reaction in that film. For dissolution with no chemical reaction, the mass per time dissolving is given by the mass flux at the surface,  $J$ , times the surface area of the solid,  $A$ . Under steady-state conditions this is equal to the

diffusional mass flux through a film of thickness,  $h$ , times the surface area:<sup>14,15</sup>

$$JA = D/hC_sA \quad (1)$$

The assumption of sink conditions gives the concentration gradient as the solubility of the drug,  $C_s$ . The diffusion coefficient is  $D$ . The maximum rate of mass reaction for an enzymic reaction within the volume  $Ah$  is:

$$r = V_{max}Ah \quad (2)$$

where  $V_{max}$  is the maximum velocity of the enzyme (in units of mass/volume/time) given by the product of the catalytic rate constant,  $K_{cat}$ , times the enzyme concentration  $E_0$ .<sup>16</sup>

The effect of an enzymatic reaction is therefore significant when the quantities in eqs. 1 and 2 are on the same order:

$$R^* = \frac{V_{max}h^2}{DC_s} \sim 1 \quad (3)$$

and becomes increasingly more significant as  $R^*$  becomes large.

Typical film thicknesses for the rotating disk apparatus described by Wood et al.<sup>17</sup> are on the order of  $2-3 \times 10^{-3}$  cm for rotational speeds in the 100-300 rpm range.<sup>18</sup> The diffusion coefficients for most compounds in dilute aqueous solutions are on the order of  $5 \times 10^{-6}$  cm<sup>2</sup>/s.<sup>19,20</sup> For the rotating disk, then, the value for  $h^2/D$  is approximately one. Therefore, for this system, an enzymatic reaction can be estimated to affect the dissolution rate of a substrate when the following relationship holds:

$$K_{cat}E_0 \geq C_s \quad (4)$$

where  $K_{cat}$  is expressed in reciprocal seconds and  $E_0$  and  $C_s$  are expressed in equivalent concentration units.

This report develops a closed form solution to the dissolution plus enzymatic reaction problem for rotating-disk hydrodynamics. The rotating-disk apparatus was chosen because the hydrodynamic theory for this system already existed<sup>16</sup> and its application to drug dissolution is well established.<sup>21,22</sup> The dissolution rates of two substrates for the proteolytic enzyme  $\alpha$ -chymotrypsin were studied. These substrates were the L-forms of 1 and 2. Both had similar catalytic rate constants, but the latter had an aqueous solubility that was two orders of magnitude lower than the former. Since the catalytic rate constant is a function of pH,<sup>23-27</sup> the reaction rate could be varied by varying both pH and enzyme concentration. It will be shown that the solubility/reaction rate dependency of the dissolution rate may be of particular pharmaceutical significance.

## Theoretical Section

**Model**—The rotating-disk apparatus is shown schematically in Fig. 1. When there is no reaction occurring in the

solution, the mass balance at steady state is given by:<sup>18</sup>

$$V_y \frac{dC}{dy} = D \frac{d^2C}{dy^2} \quad (5)$$

The concentration of mass is  $C$  and is dependent on  $y$ , the direction perpendicular to the solid compact surface (where  $y = 0$ ). Therefore,  $V_y$  is the fluid velocity in the  $y$  direction; the term on the left side of the equation represents convection while the term on the right represents diffusion. This expression is readily derived from the equation of continuity.<sup>20</sup> A major contribution by Levich<sup>18</sup> was in deriving the expression for the fluid velocity:

$$V_y = -\alpha y^2 \quad (6)$$

$$\alpha = 0.51 \omega^{3/2} \nu^{-1/2} \quad (7)$$

where  $\omega$  is the rotational speed in radians per second, and  $\nu$  is the kinematic viscosity of water. The kinematic viscosity of water at 25°C is  $\nu = 0.01 \text{ cm}^2/\text{s}$ .<sup>20</sup> The solution to eqs. 5–7, subject to the following boundary conditions:

$$C = C_s \text{ at } y = 0 \quad (8)$$

$$C = 0 \text{ as } y \rightarrow \infty \quad (9)$$

gives the Levich solution for the dissolution rate in units of flux:

$$J_L = 0.62D^{2/3} \nu^{-1/6} \omega^{1/2} C_s \quad (10)$$

By equating the dissolution rates,  $J$  and  $J_L$  of eqs. 1 and 10, one may calculate the thickness,  $h$ , needed to make the solution to a film model based on Fick's law correct for the rotating-disk apparatus.

$$h = 1.61D^{1/3} \nu^{1/6} \omega^{-1/2} \quad (11)$$

This film thickness applies only to the case of no reaction in the dissolution medium.

When, in addition to convection and diffusion, there exists a homogeneous reaction, mass balance requires inclusion of a reaction term in the continuity equation. In this case the continuity equation is written as:<sup>20</sup>

$$V_y \frac{dC}{dy} = D \frac{d^2C}{dy^2} + R \quad (12)$$

where  $R$  is the rate of production of mass expressed in units of mass per volume per time.

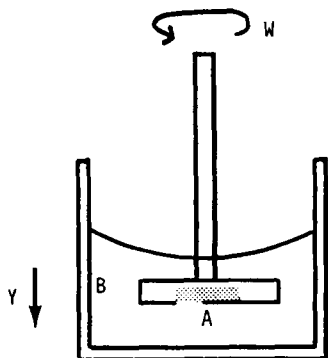
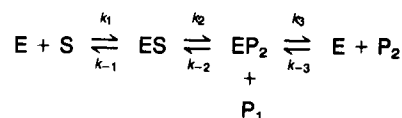


Figure 1—Diagram of the rotating-disk apparatus showing the solid compact (A) and the enzymic dissolution medium (B). The direction perpendicular to the solid surface is  $y$ .

**Kinetic Considerations**—Hydrolysis of substrates by  $\alpha$ -chymotrypsin involves association of the enzyme and substrate followed by a two-step reaction process. The kinetic scheme is represented by the following:<sup>16,28,29</sup>



Scheme 1

where, for example,  $S$  is  $N$ -benzoyltyrosine ethyl ester,  $E$  is  $\alpha$ -chymotrypsin,  $ES$  is the enzyme-substrate complex,  $P_1$  is ethanol,  $EP_2$  the acyl enzyme complex, and  $P_2$  is  $N$ -benzoyl tyrosine (i.e., the free acid). The reaction term in eq. 12 for the substrate  $S$  is thus (where in notation  $[S]$  is equivalent to  $C$ ):

$$R = k_{-1}[ES] - k_1[E][S] \quad (13)$$

The concentrations of the enzyme-substrate complex, enzyme, and substrate are represented by  $[ES]$ ,  $[E]$ , and  $[S]$ , respectively. An analytical solution is not possible for eq. 12 using this reaction term, since it contains the additional variables  $[ES]$  and  $[E]$  which are also unknown functions of  $y$ . The complete system of equations that would have to be solved are given below:

$$V_y \frac{d[S]}{dy} = D_s \frac{d^2[S]}{dy^2} - k_1[E][S] + k_{-1}[ES]$$

$$V_y \frac{d[E]}{dy} = D_E \frac{d^2[E]}{dy^2} - k_1[E][S] + k_{-1}[ES] + k_3[EP_2] + k_{-3}[E][P_2]$$

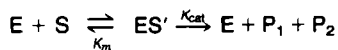
$$V_y \frac{d[ES]}{dy} = D_{ES} \frac{d^2[ES]}{dy^2} + k_1[E][S] - [k_{-1} + k_2][ES] + k_{-2}[EP_2][P_1]$$

$$V_y \frac{d[EP_2]}{dy} = D_{EP_2} \frac{d^2[EP_2]}{dy^2} + k_2[ES] - [k_{-2} + k_3][EP_2][P_1] + k_{-3}[E][P_2]$$

$$V_y \frac{d[P_1]}{dy} = D_{P_1} \frac{d^2[P_1]}{dy^2} + k_2[ES] - [k_{-2} + k_3][EP_2][P_1] + k_{-3}[E][P_2]$$

$$V_y \frac{d[P_2]}{dy} = D_{P_2} \frac{d^2[P_2]}{dy^2} + k_3[EP_2][P_1] - k_{-3}[E][P_2] \quad (14)$$

The solution to the above system of equations can only be obtained by using numerical methods. In addition, the solution is even less tractable since the individual rate constants,  $k_i$ 's, are not readily estimated or experimentally measured. Usually, enzyme kinetics are measured in terms of the simplified Michaelis-Menten kinetic scheme which consists of the formation of an enzyme-substrate complex followed by a single reaction step.<sup>16,30</sup>



Scheme II

The initial rate,  $V_0$ , is determined at various initial substrate concentrations,  $S_0$  and constant initial enzyme concentration,  $E_0$ . The Michaelis constant,  $K_m$ , and the maximum velocity ( $V_{max} = K_{cat}E_0$ ) are found by regression of the following equation:

$$V_0 = \frac{V_{max}S_0}{K_m + S_0} \quad (15)$$

Adaptation of the mechanistic Scheme I for  $\alpha$ -chymotrypsin to the experimental Scheme II gives the following relationships:<sup>16,30</sup>

$$K_m = \frac{k_3}{k_2 + k_3} K_s \quad (16)$$

$$K_{cat} = \frac{k_2 k_3}{k_2 + k_3} \quad (17)$$

$$K_s = \frac{k_{-1}}{k_1} \quad (18)$$

Using Scheme II, and assuming the final step of that scheme is rate limiting, the reaction term in eq. 12 can be written as:

$$R = -K_{cat}[ES'] \quad (19)$$

[Note: The negative sign is due to definition of  $R$  in eq. 12 as rate of production of mass.]

Equation 19 still contains a variable,  $[ES']$ , which is an unknown function of  $y$ . However, eq. 19 has the advantage over eq. 13 in that it contains  $K_{cat}$ , an easy parameter to obtain experimentally. Therefore, one can concentrate on estimating the functional form of  $[ES']$  rather than going to a system of equations such as that seen in eq. 14.

As a first approximation, one can assume that  $[ES']$  is a constant for all values of  $y$  and is equal to the enzyme concentration in the bulk medium,  $E_0$ . This initial approximation is a result of using Olander's total component balance method on all the enzyme species of the system.<sup>31</sup> Although this method estimates  $E_0$  as the upper limit for the value of  $[ES']$ , it is probable that functionally  $[ES']$  must take on a value either higher or lower than  $E_0$ . How much higher or lower is unknown and would have to be determined empirically.

With the above kinetic considerations, the reaction term is, to a first approximation, estimated as follows:

$$R = -K_{cat}E_0 \quad (20)$$

With this expression eq. 12 becomes:

$$V_y \frac{dC}{dy} = D \frac{d^2C}{dy^2} - K_{cat}E_0 \quad (21)$$

where  $V_y$  is given in eqs. 6 and 7.

**Boundary Conditions**—The boundary conditions for the problem are:

$$1. \text{ at } y = 0, C = C_s \quad (22)$$

$$2. \text{ at } y = y_0, C = 0 \quad (23)$$

The second boundary condition is a statement of sink conditions. However, unlike the case with no chemical reaction,

letting  $y$  go to infinity (see eq. 9) leads to a divergent solution. Also  $y_0$ , the reaction zone thickness, should decrease in size as the reaction rate increases. That is, the sink is brought closer to the solid surface due to the fact that a shorter reaction time allows for a shorter diffusion time. Fortunately the reaction zone thickness cannot be arbitrarily assigned and even more importantly can be derived uniquely. A mass balance reveals that all the material which dissolves reacts in the reaction zone:

$$J = \int_0^{y_0} K_{cat}E_0 dy = K_{cat}E_0 y_0$$

The reaction zone thickness is therefore determined to be:

$$y_0 = J/K_{cat}E_0 \quad (24)$$

One should not confuse  $y_0$  with  $h$  derived from a stagnant film model. In fact, it is seen in eq. 25 that as the reaction rate goes to zero, the reaction zone thickness,  $y_0$ , goes to infinity (as is the case with no reaction as solved by Levich).

**Dimensional Analysis/Solution**—It is convenient to make the problem dimensionless. This is done by letting:

$$C^* = C/C_s \quad (26)$$

$$Z = y/L \quad (27)$$

$$dZ = dy/L \quad (28)$$

$$dZ^2 = dy^2/L^2 \quad (29)$$

where  $L$  is a chosen characteristic length which is as yet unspecified. Making these substitutions (along with the appropriate expression of  $V_y$ ) into eq. 21 the following equation results:

$$\frac{d^2C^*}{dZ^2} + \frac{aL^3Z^2}{D} \frac{dC^*}{dZ} = \frac{K_{cat}E_0L^2}{C_sD} \quad (30)$$

where  $a$  is defined in eq. 7.

Putting eq. 30 into self-adjoint form:

$$\frac{d}{dZ} \left[ \exp\left(\frac{aL^3Z^3}{3D}\right) \frac{dC^*}{dZ} \right] = \frac{K_{cat}E_0L^2}{C_sD} \exp\left(\frac{aL^3Z^3}{3D}\right) \quad (31)$$

it is seen that the most convenient choice for the characteristic length  $L$  is:

$$L = \left(\frac{3D}{a}\right)^{1/3} \quad (32)$$

Substituting  $a$  from eq. 7 into eq. 32, it is found that the chosen characteristic length is 1.119 times the film thickness  $h$  derived in the film model for this system with no reaction (see eq. 11).

The dimensionless problem becomes:

$$\frac{d}{dZ} \left[ \exp(Z^3) \frac{dC^*}{dZ} \right] = 1.252R^* \exp[Z^3] \quad (33)$$

where:

$$R^* = \frac{K_{cat}E_0h^2}{C_sD} \quad (34)$$

and has the physical interpretation as explained in the introduction. The ratio  $R^*$  can be rewritten as:

$$R^* = \frac{K_{cat}E_0C_sD}{(J_L)^2} \quad (35)$$

where  $J_L$  is the Levich dissolution rate with no reaction (eq. 10).

The solution to eq. 33 gives the concentration of the substrate in dimensionless form,  $C^*$ , as a function of distance from the solid surface,  $Z$ . The solution to eq. 33 is given below, where  $C_1$  and  $C_2$  are the constants of integration:

$$C^* = 1.252R^* \int_0^Z \int_0^b \exp[s^3 - b^3] ds db + C_1 \int_0^Z \exp[-b^3] db + C_2 \quad (36)$$

The constants of integration are found through the following boundary conditions which are the dimensionless forms of eqs. 22 and 23:

$$Z = 0, C^* = 1 \quad (37)$$

$$Z = Z_0, C^* = 0 \quad (38)$$

These constants are found to be:

$$C_2 = 1 \quad (39)$$

$$C_1 = \frac{-(1 + 1.252R^* \int_0^Z \int_0^b \exp[s^3 - b^3] ds db)}{\int_0^{Z_0} \exp(-b^3) db} \quad (40)$$

The dissolution rate, written in units of flux, is given as:

$$J = -D \frac{dC}{dy} \Big|_{y=0} \quad (41)$$

In dimensionless units this is equivalent to:

$$J^* = -0.894 \frac{dC^*}{dZ} \Big|_{Z=0} = -0.894C_1 \quad (42)$$

$$J^* = J/J_L \quad (43)$$

where  $J^*$  is dissolution rate with reaction normalized to the dissolution rate under the same conditions with no reaction. Finally, to get the relationship between  $R^*$  and  $Z_0$ , eq. 24 is put in dimensionless form and equated to eq. 42. This relationship is given below:

$$\frac{1}{R^*} = 1.252 \left[ Z_0 \int_0^{Z_0} \exp[-b^3] db - \int_0^{Z_0} \int_0^b \exp[s^3 - b^3] ds db \right] \quad (44)$$

The dimensionless form of eq. 24 is:

$$J^* = 1.119 R^* Z_0 \quad (45)$$

In practice,  $R^*$  would be given,  $Z_0$  computed (eq. 44), and the flux calculated from eq. 45.

Table I gives the relationship between  $R^*$ ,  $Z_0$  and the normalized dissolution rate  $J^*$ . The values in Table I were determined by numerical integration of eq. 44 using Simpson's rule.<sup>32</sup> Notice that the dimensionless thickness,  $Z_0$ , goes to infinity as the reaction rate,  $R^*$ , goes to zero. This is

Table I—Theoretical Values for  $R^*$ ,  $Z_0$ , and  $J^*$

$R^*$	$Z_0$	$J^*$
0.0	$\infty$	1.0
0.03559	26.0	1.0277
0.04437	21.0	1.0366
0.7366	13.0	1.0724
0.27933	4.0	1.2511
0.40064	3.0	1.3405
0.68875	2.0	1.5371
1.8755	1.0	2.1000
6.5443	0.5	3.6640
17.797	0.3	5.9875
39.984	0.2	8.9455
159.62	0.1	17.8820

consistent with the boundary condition used by Levich (eq. 9).

**Limiting Case/Approximate Solution**—If the rate of reaction is large, the drug molecule cannot diffuse far from the solid surface before it will react. The reaction zone thickness,  $Z_0$ , will therefore become small with large  $R^*$ . Order of magnitude analysis approximates the diffusive and convective terms of eq. 30, respectively, below. The expression for  $L$  in eq. 32 has been substituted into eq. 30:

$$\frac{d^2C^*}{dZ^2} = \frac{\Delta C^*}{(\Delta Z)^2} = \frac{1}{Z_0^2} \quad (46)$$

$$3Z_0^2 \frac{dC^*}{dZ} = 3Z_0^2 \frac{\Delta C^*}{\Delta Z} = 3Z_0 \quad (47)$$

The ratio of the convective term to the diffusive term is therefore equal to  $3Z_0$  which is very small for large  $R^*$  values. Therefore, the convective term is negligible with high reaction rates. This is because the fluid velocity is proportional to the distance from the solid surface squared (see eq. 6) and that distance is never large within the small reaction zone associated with a rapid reaction.

The continuity equation (eq. 30) in this limiting case is:

$$\frac{d^2C^*}{dZ^2} = 1.252R^* \quad (48)$$

Solving this equation along with the boundary conditions of eqs. 37 and 38 and using the relationship of  $R^*$  and  $Z_0$  given by eq. 45 gives:

$$J^* = (2R^*)^{1/2} \quad (49)$$

It can be shown that this function is the limit of the previous solution (eqs. 44 and 45) for large  $R^*$  values. At a value of  $R^*$  equal to 1.9, the solution of eq. 49 is within 8% of the full solution and is already within 1% at an  $R^*$  value of 6.5.

Because the solution given by eqs. 44 and 45 are somewhat difficult to use in practice, an approximation to that solution was sought. It was found empirically that the solution given below approximates the solution within 4% for all  $R^*$  values:

$$J^* = \frac{1}{1 + 2.16(R^*)^{0.58}} + (2R^*)^{1/2} \quad (50)$$

A graph of the normalized dissolution rate versus  $R^*$ , the dimensionless reaction rate, is given in Fig. 2.

By setting the solution of eq. 50 for dissolution rate, with reaction equal to an expression similar to eq. 1, the film thickness for a model with reaction using film theory can be obtained. Doing this, it is found that the ratio of the film

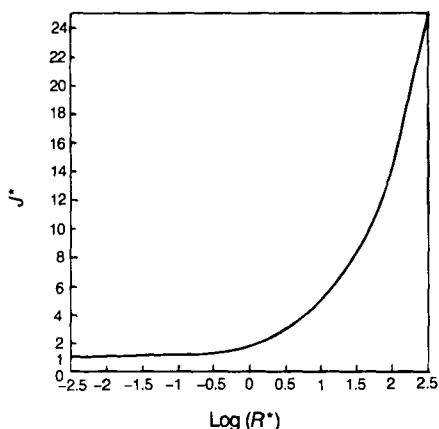


Figure 2—Theoretical plot of  $J^*$ , the dissolution rate with reaction divided by the dissolution rate predicted by Levich for no reaction, versus the logarithm of  $R^*$ , the reaction rate parameter.

thickness with reaction,  $h_R$ , to that with no reaction (see eq. 11) is the reciprocal of eq. 50:

$$\frac{h_R}{h} = \frac{1 + 2.16(R^*)^{0.58}}{1 + (2R^*)^{1/2} [1 + 2.16(R^*)^{0.58}]} \quad (51)$$

which is always  $\leq 1$ . These film thicknesses are given because it is common to see, especially in the pharmaceutical literature, mass fluxes expressed in a form similar to eq. 1. When these thicknesses are known exactly, it is usually because an expression such as eq. 1 is set equal to a solution from a convective-diffusive problem, as was done in this paper for the rotating disk. More often than not, the thicknesses are unknown since most systems are hydrodynamically more complex than the rotating disk and the solution to the corresponding convective-diffusive problem does not exist.

## Experimental Section

**Materials**—*N*-acetylphenylalanine, *N*-acetylphenylalanine ethyl ester (1), *N*-benzoyltyrosine ethyl ester (2), (Sigma Chemical Co., St. Louis, MO) and *N*-benzoyltyrosine (U.S. Biochemical Corp., Cleveland, OH), were obtained in pure crystalline L-form and used as received. The enzyme  $\alpha$ -chymotrypsin (Sigma Chemical Co., St. Louis, MO) was crystallized three times. Enzymic solutions were made with Tris (Sigma Chemical Co., St. Louis, MO) buffer using deionized water (Milli-Q, Continental Water Systems, El Paso, TX) which was deaerated using a slightly reduced pressure for  $\sim 30$  min or more. The enzyme solutions contained 0.05 M Tris buffer as well as 0.05 M calcium chloride. The activity of the enzyme was checked periodically with a spectrophotometric titration method utilizing *N*-trans-cinnamoylimidazole (Sigma Chemical Co., St. Louis, MO).<sup>39</sup>

**Dissolution Experiments**—The rotating disk used was similar to the one described by Wood et al.<sup>17</sup> The diameter of the disk was 3.8 cm and had a die cavity in its center whose diameter was 1.1 cm. The compounds studied were compressed directly in this disk at a pressure of 7,000 psi which was maintained for 3–4 min. The disk was rotated at various speeds using a motor equipped with a constant speed control unit (Cole-Parmer Instrument Co., Chicago, IL). The rotational speed was calibrated and monitored repeatedly throughout each dissolution experiment using a tachometer (Cole-Parmer Instrument Co., model 8213-20). The dissolution cell consisted of a jacketed beaker maintained at  $25 \pm 0.1^\circ\text{C}$ . The dissolution media was the enzyme solution described above and had enzyme concentrations that ranged from 0 to  $2.4 \times 10^{-8}$  M. The dissolution volume was 250 mL. Each dissolution experiment was carried out for a 30-min period. Steady state occurred in  $< 10$  min. A 200- $\mu\text{L}$  sample was taken periodically and assayed for both ester and free acid forms of the compounds using reversed-phase HPLC (Kratos, Ramsey, NJ, models 773 and 400). The mobile phase was 35:65, MeOH:H<sub>2</sub>O, adjusted to pH 2.1 using phosphoric acid. It was found that when no

enzyme was present, aqueous hydrolysis of the ester was negligible within the time frame of the experiment. Also, even the smallest concentration of enzyme ( $\sim 10^{-8}$  M) would cause complete hydrolysis of the ester within the time frame of sampling, although the reaction rate was too slow to affect the dissolution rate. Therefore, if any enzyme were present, only free acid would be detected in the sample.

In addition to varying enzyme concentration, the rotational speed was varied and, in the case of 2, the pH was also varied from 7.0 to 7.8 in increments of 0.2  $\pm$  0.05 pH units (Radiometer, Copenhagen, Denmark, model PHM 64).

**Diffusion Coefficients**—The diffusion coefficients were obtained by measuring the dissolution rates as a function of rotational speed with no enzyme present. A least-squares regression was applied to the Levich solution of eq. 10. The values for the diffusion coefficients obtained in this manner were  $6.98 \pm 0.08 \times 10^{-6}$  and  $4.94 \pm 0.04$  cm<sup>2</sup>/s for compounds 1 and 2, respectively.

**Solubility**—The aqueous solubility was measured by placing excess solid in vials containing deionized water. The vials were placed in a water bath at  $25 \pm 0.1^\circ\text{C}$ . The vials were vortexed three times daily. After a sufficient time, samples were removed, filtered, and diluted 1:10. The ester concentration was determined by HPLC assay. Samples were assayed daily for 1 week. Solubilities measured after 48 h were not found to be significantly different than those measured after 1 week. Compound 2 had a measured solubility of  $4.66 \pm 0.06 \times 10^{-4}$  M while 1 had a value nearly two orders of magnitude higher,  $1.38 \pm 0.05 \times 10^{-2}$  M.

**Kinetic Experiments**—For compound 1, the value  $160 \text{ s}^{-1}$  for  $K_{\text{cat}}$  at pH 7.8 reported by Hammond and Gutfreund<sup>34</sup> was used. For 2, Bender et al.<sup>35</sup> reported a value for  $K_{\text{cat}}$  of  $200 \text{ s}^{-1}$  at pH 7.8. However, the dissolution of this compound was studied at various pH values and, therefore, the catalytic rate constant had to be determined at each of these pH values.

The method used to measure the reaction rates was the modified spectrophotometric method described by Hummel.<sup>36</sup> The spectrophotometer used was a Perkin-Elmer Lambda 3B equipped with a model 3600 data station. The spectrophotometer was fitted with jacketed cell holders to maintain a constant temperature of  $25 \pm 0.1^\circ\text{C}$ . The enzyme concentrations were  $10^{-8}$  M. The initial substrate concentrations were in the range from 30 to 600  $\mu\text{M}$ , the lowest concentration being at least two times the  $K_m$  value. This gave greater reproducibility for determining  $V_{\text{max}}$  and, hence,  $K_{\text{cat}}$ . In order to avoid solubility problems, 2% (v/v) acetonitrile was added to the substrate solution. A weighted least-squares linear-regression analysis was done on the single reciprocal plot of the data:<sup>37,38</sup>

$$\frac{S_0}{V_0} = \frac{K_m}{V_{\text{max}}} + \frac{S_0}{V_{\text{max}}} \quad (52)$$

where  $S_0$  is the initial substrate concentration and  $V_0$  is the initial rate. Equation 52 can be derived from eq. 15.

## Results and Discussion

From the theoretical analysis, the variables of interest are solubility, the kinetic rate constant, the enzyme concentration of the bulk medium, and the rotational speed of the disk. The two compounds studied have very different solubilities but very similar  $K_{\text{cat}}$  values. For these two compounds, the dissolution rates were studied under conditions of varying concentrations of enzyme in the bulk medium and varying rotational speeds of the disk. For compound 2, the pH of the dissolution medium was also varied. This was another way of varying the magnitude of the enzymatic reaction since  $K_{\text{cat}}$  for  $\alpha$ -chymotrypsin hydrolysis is pH dependent.

The experimental results are given in Tables II–V. The experiments utilizing 2 were repeated at least three times and, therefore, the mean and SD are reported. Experiments with 1, on the other hand, were run only one time.

**Solubility Dependence**—The difference found experimentally between the two compounds is fairly evident. While the catalytic rate constants for these compounds are nearly the same, the solubilities differ greatly. Compound 1 has a much higher solubility and, therefore, enzymatic reaction has little

**Table II—Dissolution Rate Data for *N*-Benzoyltyrosine Ethyl Ester and *N*-Acetylphenylalanine Ethyl Ester with no Enzyme in the Bulk Medium ( $E_0 = 0$ ) and Varying rpm at pH = 7.8**

rpm	$J_L \times 10^9$ (mol/cm <sup>2</sup> /s) $\pm$ SD	
	<i>N</i> -Benzoyltyrosine Ethyl Ester	<i>N</i> -Acetylphenylalanine Ethyl Ester <sup>a</sup>
100	0.599 $\pm$ 0.064	—
125	—	23.68
150	0.713 $\pm$ 0.029	—
200	0.836 $\pm$ 0.031	30.82
250	0.916 $\pm$ 0.064	34.40
300	1.005 $\pm$ 0.061	37.62

<sup>a</sup> Average of two points.

**Table III—Dissolution Rate Data for *N*-Benzoyltyrosine Ethyl Ester and *N*-Acetylphenylalanine Ethyl Ester with Constant rpm and Varying Enzyme Concentration at pH = 7.8**

<i>N</i> -Benzoyltyrosine Ethyl Ester (rpm = 200)		<i>N</i> -Acetylphenylalanine Ethyl Ester (rpm = 125)	
$E_0 \times 10^{-5}$ M	$J^* \pm$ SD	$E_0 \times 10^{-5}$ M	$J^* \pm$ SD
0.347	2.89 $\pm$ 0.01	0.398	1.011
0.695	3.78 $\pm$ 0.19	0.796	1.021
1.045	4.22 $\pm$ 0.17	1.194	1.040
1.389	4.40 $\pm$ 0.35	1.554	1.046
1.736	4.573 $\pm$ 0.19	1.592	1.051
2.39	5.550 $\pm$ 0.39	2.030	1.067
—	—	2.33	1.074
—	—	3.18	1.113

<sup>a</sup> Experimentally determined dissolution rate normalized to the dissolution rate with no reaction as predicted by eq. 10. <sup>b</sup> Single point determination.

**Table IV—Dissolution Rate Data for *N*-Benzoyltyrosine Ethyl Ester and *N*-Acetylphenylalanine Ethyl Ester with Constant Enzyme Concentration and Varying rpm at pH = 7.8**

rpm	$J^* \pm$ SD	
	<i>N</i> -Benzoyltyrosine Ethyl Ester <sup>b</sup>	<i>N</i> -Acetylphenylalanine Ethyl Ester <sup>c,d</sup>
100	7.44 $\pm$ 0.25	—
125	—	1.067
150	6.36 $\pm$ 0.26	—
200	5.55 $\pm$ 0.39	1.046
250	5.62 $\pm$ 0.17	0.997
300	5.18 $\pm$ 0.15	1.001

<sup>a</sup> Experimentally determined dissolution rate normalized to the dissolution rate with no reaction as predicted by eq. 10. <sup>b</sup>  $E_0 = 2.39 \times 10^{-5}$  M. <sup>c</sup>  $E_0 = 2.03 \times 10^{-5}$  M. <sup>d</sup> Single point determination.

**Table V—Dissolution Rate Data for *N*-Benzoyltyrosine Ethyl Ester with Constant Enzyme Concentration ( $E_0 = 2.39 \times 10^{-5}$  M), Constant Rotational Speed (rpm = 200), and with Varying pH**

pH	$J \times 10^9$ (mol/cm <sup>2</sup> /s) $\pm$ SD
7.8	4.59 $\pm$ 0.32
7.6	3.76 $\pm$ 0.40
7.4	3.32 $\pm$ 0.42
7.2	2.93 $\pm$ 0.11
7.0	2.63 $\pm$ 0.12

impact on dissolution. With high solubility, the dissolution rate is also very high even without reaction, as predicted by the Levich solution. It would, therefore, take a fast reaction rate to consume the entire mass undergoing dissolution within a small reaction zone. As seen in eq. 34, it would take extraordinarily high  $K_{cat}$  and/or bulk enzyme concentrations to give large  $R^*$  values for highly soluble drugs.

The dissolution rate with no reaction depends on the solubility to the first power. However, examining the limiting-case solution with high reaction (see eq. 49), it is seen that the dissolution rate is proportional to the solubility to the one-half power. When all substitutions are made, eq. 49 is equivalent to the following expression:

$$J = [2K_{cat}E_0DC_s]^{1/2} \quad (53)$$

Examination of the solubility dependency can be made for 1 and 2 by considering experiments performed under similar conditions. The dissolution rate can be expressed as (see eqs. 50 and 51):

$$J = J_L \cdot \frac{h}{h_R} \quad (54)$$

It should be noted that  $h/h_R$  by definition is equal to  $J^*$  and, under conditions of no reaction, is equal to 1. Since the diffusion coefficients of 1 and 2 are similar, the ratio of the dissolution rates at a given rpm with no enzyme should be approximately equal to the ratio of the solubilities of 1 and 2 (compare data of Table II with similar rpm). The solubility of 2 is 1/30th of the solubility of 1. In the presence of reaction, however, the ratio of the dissolution rates under similar conditions is equal to the ratio of the solubilities times the ratio of the  $h/h_R$  values. The data in Table IV (relevant since  $K_{cat}$  is approximately the same for 1 and 2, and enzyme concentrations are approximately equal) reveal that at a given rpm, 200 for example, the ratio of the dissolution rates is close to the ratio of the square roots of the solubilities, as might be expected from the limiting-case solution of eq. 53 [(1/30)(5.55/1.046) = 0.18]. The square root of the solubility ratio is (1/30)<sup>1/2</sup> = 0.18. This clearly shows that the decrease in the dissolution rate due to a lowering of the solubility will be significantly reduced in the presence of an enzymatic reaction.

The importance of the solubility dependence is understood when one considers the effect of making a prodrug whose solubility is orders of magnitude less than its parent drug. Ordinarily this means a decrease in dissolution rate proportional to the solubility decrease (see eq. 1). While in some cases this effect may be desired for prolonged release,<sup>3</sup> in other cases the decrease in dissolution rate may be detrimental to bioavailability. An enzymatic reaction may, however, compensate for this decrease in dissolution rate with solubility. As seen in Fig. 2, it is possible that this compensation may reasonably be from one to perhaps two orders of magnitude. In fact it is possible that while the prodrug derivative may have a lower solubility than its parent, it may actually have a faster dissolution rate if  $R^*$  is large enough.

Applications of the above principle are particularly interesting in considering suspension formulations. Suspensions degrade via zero-order kinetics and the rate constant is proportional to the drug solubility. Making a prodrug with a solubility orders of magnitude lower will increase shelf-life stability tremendously. If the prodrug is made as a substrate for one of the digestive enzymes, rapid dissolution and bioreconversion may result on oral administration.

**Bulk Enzyme Concentration Dependence**—At pH 7.8, the rotational speed was kept at a constant value while the

enzyme concentration was varied. The results for 2 are shown graphically in Fig. 3. The theoretical curve was calculated using the literature value for  $K_{\text{cat}}$  ( $200 \text{ s}^{-1}$ ).<sup>36</sup> Good agreement between the theory and the experiments exists. Calculation of  $R^*$  values show most of the data to be in the limiting-case region. From eq. 53 it is seen that, in the limiting case, the dissolution rate is proportional to the enzyme concentration to the one-half power.

**Rotational Dependence**—At a constant enzyme concentration, the rpm was varied. Figure 4 shows the results for 2. The increase in dissolution rate due to reaction is greater for slower rotational speeds. This is due to the fact that at slower speeds the boundary-layer thickness is increased. The drug has a longer time to diffuse and, hence, a greater probability of reacting within the reaction zone.

The pharmaceutical implications are two-fold. First, if the reaction is fast, the dissolution rate is independent of the hydrodynamics. An interphase transport problem with no reaction is a convective-diffusive problem. With a large reaction term, the problem becomes one of reaction-diffusion. Interphase transport rates become more dependent on the reaction rate and less dependent on the sometimes unknown hydrodynamics of the system. Examination of the limiting

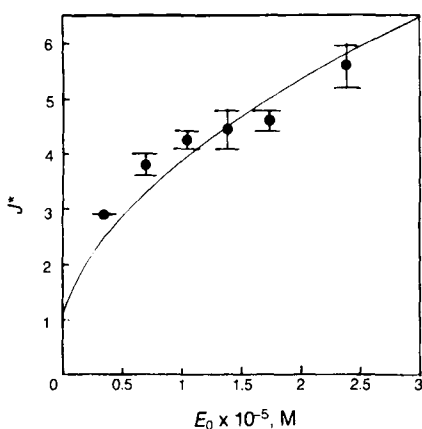


**Figure 3**—The normalized dissolution rate,  $J^*$ , of *N*-benzoyltyrosine ethyl ester versus the enzyme concentration  $E_0$ . The solid line is the theoretical curve predicted by eq. 50. The error bars represent the SD of the experimental data.

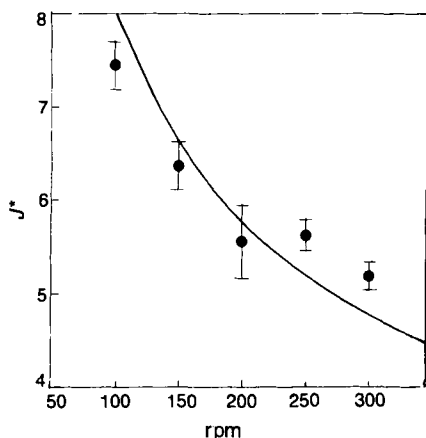


**Figure 4**—The normalized dissolution rate,  $J^*$ , of *N*-benzoyltyrosine ethyl ester versus the rotational speed. The solid line is predicted by theory and error bars represent the SD. The curve shows that the increase in dissolution rate due to reaction decreases as convection increases.

case solution reveals the lack of the rotational speed variable (see eq. 53).

Secondly, a reaction does not have to be as rapid in a system with no convection in order to influence interphase transport rates. This suggests the possibility of incorporating a chemical reaction in a hydrogel or other polymeric phase for the purpose of chemically controlled delivery. The effect of a homogeneous chemical reaction in the biophase of the skin has already been shown to greatly effect the transdermal absorption of drugs.<sup>39</sup>

**pH Dependence**—The catalytic rate constant for the hydrolysis of esters varies with pH.<sup>23-27</sup> There are two ionizable groups of  $\alpha$ -chymotrypsin whose states of ionization are important in terms of the activity of  $\alpha$ -chymotrypsin. One is the imidazole group of histidine located at the active site and the other is the amino group of the terminal isoleucine. The result of these two ionizable groups is that the enzyme has optimum activity around  $\text{pH} = 7.8$ .<sup>16,24</sup> The isoleucine residue has a  $\text{p}K_a$  value of  $\sim 9.23$ ; therefore, in the range of pH for the dissolution studies, consideration will be given only to the ionization of the histidine residue. The dependence of  $K_{\text{cat}}$  on pH is given below for the rate-limiting case where deacylation of the acyl enzyme intermediate is the rate-limiting step ( $k_2 \gg k_3$ ). This would be the case for ester substrates of  $\alpha$ -chymotrypsin.<sup>26</sup>

$$(K_{\text{cat}})_{\text{pH}} = \frac{k_3}{1 + \frac{[\text{H}^+]}{K_a}} \quad (55)$$

where  $K_a$  is the ionization constant for the histidine residue.

The values of  $K_{\text{cat}}$  for 2 were determined from pH 7.0 to 7.8. They are presented in Table VI. The Michaelis-Menten constant,  $K_m$ , was found to be 0.016 mM with an SD of 0.005 and was, as expected, found to be independent of pH val-

**Table VI**—Experimental Kinetic Rate Constant,  $K_{\text{cat}}$ , for *N*-Benzoyltyrosine Ethyl Ester at Various pH values

pH	$K_{\text{cat}} (\text{s}^{-1}) \pm \text{SD}$
7.8	$150 \pm 10.0$
7.6	$125 \pm 9.6$
7.4	$102 \pm 7.5$
7.2	$91 \pm 6.6$
7.0	$68 \pm 4.3$

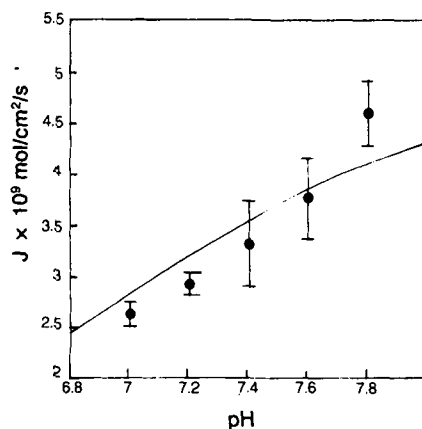


**Figure 5**—The dissolution rate of *N*-benzoyltyrosine ethyl ester versus pH. The theoretical solid line is calculated from the solution in eq. 50 using eq. 54 for the dependence of the catalytic rate constant on pH. The error bars represent the SD of the experimental data points.

ue.<sup>24,26</sup> A least-squares regression of the data in Table VI according to eq. 55 gave  $K_3 = 191 \text{ s}^{-1} \pm 11.5 \text{ SD}$  and  $\text{p}K_a = 7.27 \pm 0.025 \text{ SD}$ . The  $\text{p}K_a$  determined was slightly higher than the value found by others:  $\text{p}K_a = 6.7$ ;<sup>24,29</sup>  $6.9$ ;<sup>25</sup>  $7.14$ .<sup>40</sup>

The dissolution rate for 2 versus pH is shown in Fig. 5. The theoretical curve was calculated from the solution and by using the function in eq. 55 for  $K_{\text{cat}}$ . It is seen that the theory is in agreement with the experiments.

In the previous figures, the  $K_{\text{cat}}$  at  $\text{pH} = 7.8$  used to calculate the theoretical curves was  $200 \text{ s}^{-1}$ , i.e., the value reported by Bender et al.,<sup>36</sup> and not  $150 \text{ s}^{-1}$  as determined in the present kinetic studies (see Table VI). Least-squares regression analysis on all the data for 2 listed in Tables III and IV resulted in a catalytic rate constant of  $K_{\text{cat}} = 206 \text{ s}^{-1}$ . Although there is some discrepancy between using the values 200 and 150, most theoretical values of the dissolution rates calculated using  $K_{\text{cat}} = 150 \text{ s}^{-1}$  are 87% of those using  $K_{\text{cat}} = 200 \text{ s}^{-1}$ . This is due to the fact that at fast reaction rates the dissolution rate is proportional to  $K_{\text{cat}}$  to the one-half power as was shown in eq. 53. Table VII compares all the pH 7.8 data for 2 to the dissolution rate predicted when the dissolution rate predicted depends on the choice of the value for  $K_{\text{cat}}$ . Even for the less favorable choice of  $K_{\text{cat}}$  ( $150 \text{ s}^{-1}$ ), the agreement seems good, considering the complexity of the problem and the simplicity of the solution.

**Comparison of Theory and Experiments**—Because of the simplifying assumptions made and because of the powerful use of dimensional analysis, the solution consists of only two variables,  $R^*$  and  $J^*$ . This makes it possible to represent all the data for all compounds on one curve (as was seen in Fig. 2). All the data for 1 and 2 in Tables III–V are shown graphically in Fig. 6. Again, what is most readily apparent is that the dissolution rate of the higher solubility compound, 1, was only slightly affected by the presence of the enzymatic reaction. Although a perfect fit is not seen for all the data, the overall trend is apparent.

Deviation of the experimental results from the theory may have many explanations. One is in the approximation of the concentration profile for the enzyme–substrate complex,  $\text{ES}'$  (eqs. 19 and 20). Functionally, one can keep the concentration of the species constant throughout the reaction zone. However, the correct constant value needed to make the solution to the differential equation correct is unknown and will probably depend on all the parameters of the system. As a first approximation, this constant was chosen to be equal to the concentration of the enzyme in the bulk medium. Analyzing the data for both the compounds studied, no real correlation in the deviations with rotational speed or bulk enzyme concentration could be found. However, it is obvious from Fig. 6 that the experimental data for 1, which has the higher

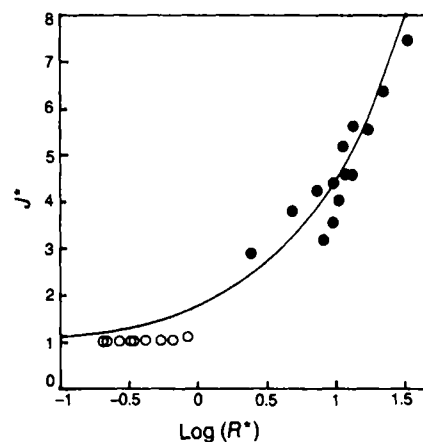


**Figure 6**—The normalized dissolution rate versus the logarithm of the reaction parameter,  $R^*$ , for *N*-acetylphenylalanine ethyl ester (●), and *N*-benzylytyrosine ethyl ester (○). The difference, due to the relative solubilities of the two compounds, is clearly shown. Data are for all rotational speeds, bulk enzyme concentrations, and pH values.

aqueous solubility, were consistently lower than theoretical predictions. This indicates that the concentration of enzyme in the bulk medium overestimates the enzyme–substrate complex concentration. It seems that as the reaction zone gets larger (i.e.,  $R^*$  gets smaller, which in this case is due to the high solubility) the enzyme–substrate complex concentration should be estimated to be some fraction of the bulk enzyme concentration. In this region, however, the increase in dissolution rate due to enzymatic reaction is small, whether one considers the experimental data or the theoretical prediction.

Another consideration is that one product of the esterolysis is a carboxylic acid which ionizes due to the relatively high pH. This liberation of hydronium ions may result in a pH gradient within the reaction zone;<sup>9</sup> therefore, the catalytic rate constant,  $K_{\text{cat}}$ , may also vary within the reaction zone.

Further insight into these deviations could be obtained from a numerical solution to the complete set of continuity equations (eq. 14). However, given the numeric difficulties inherent in a boundary value problem of this system size and the number of parameters involved, it appears that a numerical solution may not provide more insight than the simple solution obtained here.

## Conclusions

Enzyme reactions were determined to be large enough to affect the dissolution rate of a solid substrate. Dimensional analysis led to the definition of the single most important parameter,  $R^*$ , which determines the relative importance of the reaction rate in regard to the diffusional process. This parameter may be simply regarded as the ratio of the diffusion time to the reaction time<sup>10</sup> when these times are defined as follows:

$$t_R = \frac{C_s}{V_{\text{max}}} \quad (56)$$

$$t_D = \frac{h^2}{D} \quad (57)$$

The dimensionless parameter  $R^*$  is obtained from a model using simplifying assumptions in regard to the kinetic scheme. An analytical solution to the true system (eq. 14) is not possible. It is believed that a numeric solution to that system would not produce as good a qualitative description as

**Table VII**—Comparison of all the Experimental Dissolution Rates at pH 7.8 for *N*-Benzylytyrosine Ethyl Ester to the Predicted Dissolution Rates Which are Calculated from Equation 50 Using  $K_{\text{cat}} = 150$  and  $200 \text{ s}^{-1}$

$(R^*/K_{\text{cat}}) \times 10^2$	$J_{\text{exp}}/J_{\text{pred}}$	
	$(K_{\text{cat}} = 150)$	$(K_{\text{cat}} = 200)$
1.17	1.36	1.21
2.34	1.33	1.17
3.52	1.24	1.08
4.68	1.13	0.99
5.37	1.25	1.09
5.85	1.06	0.93
6.44	1.25	1.09
8.06	1.11	0.96
10.74	1.10	0.96
16.11	1.06	0.92

the  $R^*$  parameter model. The latter model was found to correctly predict the trends found experimentally. Perhaps the most pharmaceutically significant parameters in  $R^*$  are the solubility and  $K_{cat}$ . The catalytic rate constants for ester hydrolysis by  $\alpha$ -chymotrypsin are on the order of  $100\text{--}200\text{ s}^{-1}$  while amide hydrolysis is on the order of  $1\text{ s}^{-1}$ . The model, therefore, suggests that in certain prodrug strategies an ester derivative may possess a particular advantage over an amide derivative.

Experimentally it was found that increases in dissolution rates due to enzymatic reaction for 1 were much slower than the less soluble 2. This is due to the fact that highly soluble compounds already have a fast rate of dissolution. It was concluded that the decrease in dissolution rate due to a prodrug derivative whose solubility is lower than the parent drug may be compensated for by the presence of an enzymatic reaction, if the prodrug is an amino acid derivative which serves as a substrate for the enzyme. It is further concluded that although highly soluble compounds may not have their dissolution rates increased significantly by chemical reaction, there may be a significant effect on the interphase transport rates from a medium in which the concentration of the compound is kept low. An example would be the release of a substrate from a polymer phase into a surrounding enzyme solution.

A final conclusion is that the model predicts the possibility of reaction-controlled interphase transport. It is seen that the solution goes from convectively controlled diffusion to one of reaction-controlled transport. Experimentally it was shown that as the rotational speed of the disk was decreased (convection decreased), the impact of enzymatic reaction on dissolution rate increased.

## References and Notes

- Higuchi, W. I.; Nelson, E.; Wagner, J. G. *J. Pharm. Sci.* 1964, 53, 333-335.
- Hamlin, W. E.; Higuchi, W. I. *J. Pharm. Sci.* 1966, 55, 205-207.
- Higuchi, T.; Lee, H. K.; Pitman, I. H. *Farm. Aikak* 1971, 80, 55-90.
- Andersgaard, H.; Finholt, P.; Gjermunsen, R.; Hoyland, T. *Acta Pharm. Suec.* 1974, 11, 239-248.
- Higuchi, T.; Stella, V. J. "Prodrugs as Novel Drug Delivery Systems", ACS Symposium Series 14; American Chemical Society: Washington, DC, 1975; pp 51-66.
- Donbrow, M.; Touitou, E. *J. Pharm. Pharmacol.* 1977, 29, 524-528.
- Lee, H. K.; Lambert, H.; Stella, V. J.; Wang, D.; Higuchi, T. *J. Pharm. Sci.* 1979, 68, 288-295.
- Mooney, K. G.; Mintun, M. A.; Himmelstein, K. J.; Stella, V. J. *J. Pharm. Sci.* 1981, 70, 13-22.
- Mooney, K. G.; Mintun, M. A.; Himmelstein, K. J.; Stella, V. J. *J. Pharm. Sci.* 1981, 70, 22-32.
- Mooney, K. G.; Rodriguez-Gaxiola, M.; Mintun, M. A.; Himmelstein, K. J.; Stella, V. J. *J. Pharm. Sci.* 1981, 70, 1358-1365.

- Touitou, E.; Donbrow, M. *Int. J. Pharm.* 1981, 9, 97-106.
- Hirotsune, I.; Carey, M. C. *J. Lipid Res.* 1981, 22, 254-270.
- Amidon, G. L.; Pearlman, R. S.; Leesman, G. D. "Design of Biopharmaceutical Properties Through Prodrugs and Analogs"; American Pharmaceutical Association: Washington, DC, 1977; pp 281-315.
- Noyes, A. A.; Whitney, W. R. *J. Am. Chem. Soc.* 1897, 19, 930-934.
- Nernst, W. *Z. Physik. Chem.* 1904, 47, 52-55.
- Gray, C. J. "Enzyme-Catalysed Reactions"; Van Nostrand Reinhold: London, 1971; pp 72-74, 148-166.
- Wood, J. H.; Syrato, J. E.; Letterman, H. *J. Pharm. Sci.* 1965, 54, 1068.
- Levich, V. G. "Physicochemical Hydrodynamics"; Prentice-Hall: Englewood Cliffs, NJ, 1962; pp 60-72.
- Longworth in "American Institute of Physics Handbook" 3rd ed.; McGraw Hill: New York, NY, 1972, pp 221-229.
- Bird, R. B.; Stewart, W. E.; Lightfoot, E. N. "Transport Phenomena"; Wiley: New York, 1960; pp 8, 502-516, 559.
- Prakongpan, S.; Molokhia, A. H.; Kwan, K. H.; Higuchi, W. I. *J. Pharm. Sci.* 1976, 65, 685-689.
- Tsuji, A.; Nakashima, E.; Hamano, S.; Yamana, T. *J. Pharm. Sci.* 1978, 67, 1059-1066.
- Cunningham, L. W.; Brown, C. S. *J. Biol. Chem.* 1956, 221, 287-299.
- Bender, M. L.; Clement, G. E.; Kezdy, F. J.; Heck, H. *J. Am. Chem. Soc.* 1964, 86, 3680-3689.
- Kaplan, H.; Laidler, K. J. *Can. J. Chem.* 1967, 45, 547-557.
- Martinek, K.; Yatsimirskii, A. K.; Berezin, I. V. *Mol. Biol. (Moscow)* 1971, 5, 96-109.
- Casado, J.; Seoane, F.; Cachaza, J. M. *Rev. Roum. Chim.* 1979, 24, 1451-1456.
- Gutfreund, H.; Sturtevant, J. M. *Biochem. J.* 1956, 63, 656-661.
- Gutfreund, H.; Sturtevant, J. M. *Proc. Natl. Acad. Sci. USA* 1956, 42, 719-728.
- Segel, I. H. "Enzyme Kinetics"; Wiley-Interscience: New York, 1975; pp 29-34.
- Olander, D. R. *AIChE J.* 1959, 6, 233-239.
- MACC, "Numerical Integration Routines"; University of Wisconsin: Madison, WI, 1976.
- Schonbaum, G. R.; Zerner, B.; Bender, M. L. *J. Biol. Chem.* 1961, 236, 2930-2935.
- Hammond, B. R.; Gutfreund, H. *Biochem. J.* 1955, 61, 187-189.
- Bender, M. L.; Schonbaum, G. R.; Hamilton, G. A. *J. Polym. Sci.* 1961, 49, 75-103.
- Hummel, B. C. W. *Can. J. Biochem. Physiol.* 1959, 37, 1393-1399.
- Connors, K. A. *Interest* 1984, 23, 1-61.
- Connors, Kenneth A., personal communication.
- Yu, C. D.; Fox, J. L.; Ho, N. F. H.; Higuchi, W. I. *J. Pharm. Sci.* 1979, 68, 1341-1346.
- Kezdy, F. J.; Bender, M. L. *Biochemistry* 1962, 1, 1097-1106.

## Acknowledgments

The authors greatly appreciate the theoretical discussion with Dr. E. N. Lightfoot, of the University of Wisconsin, during the early stages of the project.

Abstracted from a dissertation submitted by D. A. Johnson to the University of Wisconsin-Madison, in partial fulfillment of the Doctor of Philosophy degree requirements.

Supported in part by the SmithKline Beckman Corp. and INTER, Research Corp.